12th International Congress on the Deterioration and Conservation of Stone
Columbia University, New York, 2012

MULTIDISCIPLINARY CHARACTERIZATION OF GYPSUM CRUST ON LEDE STONE (BELGIUM)

Tim De Kock[1,4,a], Jan Dewanckele[1,4], Marijn Boone[1,4], Laszlo Vincze[2], Gilles Fronteau[3], Luc Van Hoorebeke[4,5], Patric Jacobs[1,4] and Veerle Cnudde[1,4]

[1] UGCT- Research Group Sedimentary Geology and Engineering Geology, Department of Geology and Soil Science, Faculty of Sciences, Ghent University, Belgium.
Corresponding author: Tim.DeKock@UGent.be
[2] X-Ray Microspectroscopy and Imaging, Department of Analytical Chemistry, Faculty of Sciences, Ghent University, Belgium
[3] University of Reims Champagne-Ardenne (URCA), GEGENAA, EA3795, Reims, France
[4] UGCT- Radiation Physics Research Group, Department of Physics and Astronomy, Faculty of Sciences, Ghent University, Belgium

Abstract

The Lede stone is an arenaceous limestone which occurs in marine sandy deposits (Lede Formation, Eocene, Tertiary; Belgium). Its framework consists of quartz grains, micro- and macrofossils, glauconite and a low percentage of dense minerals such as apatite and zircon. It is commonly characterized by a microsparitic cement of calcite. Since Roman times the Lede stone was used as a building material and is dominantly present in Gothic architecture. Nowadays, huge amounts of this stone are found in the Belgian built cultural heritage, thus being the subject of many restoration and renovation works.

Since it has an substantial carbonate content, the stone is sensitive to sulphation. This causes formation of a gypsum crust and the dissolution of calcite cement towards the inside of the stone. At the same time cracks can develop during long-time atmospheric exposure. In this way, the subsurface can be divided in several zones, each with their degree of alteration. When a stone surface is cleaned during restoration works, it is important to know the structure of the gypsum crust and the cracks, the depth of the affected area and the stability conditions of each of the subsurface zones. A multidisciplinary case-study was performed on a Lede stone with a thin gypsum crust. The structure and composition of the superficial crust as well as the subsurface were studied with different techniques (X-ray tomography/radiography, X-ray fluorescence, scanning electron microscopy and optical microscopy) to determine the degree of weathering. Chemical alteration shows to be the most ‘common’ zonation with a superficial black crust layer, a second thicker gypsum alteration zone and the sound stone in the deeper part of the stone. Sub-horizontal cracks are present within both the gypsum crust and the sound stone.

Keywords: Lede stone, black crust, microstructure, alteration, X-ray microcomputed tomography

1. Introduction

Natural building stones are known to alter their surface properties when used and exposed to atmospheric conditions (e.g. Winkler, 1994; Siegesmund *et* al., 2002; Kourkoulis, 2006; Přikryl & Smith, 2007). This is the result of an interaction between the stone and its environment. As many processes can interfere with each other, the eventual alteration pattern may be very complex and will evolve through time. A first distinction in these alternation patterns can be made between erosional and depositional weathering forms. Erosional weathering eventually removes material from the stone (e.g. flaking, dissolution, exfoliation) while depositional weathering adds material to the stone's surface (e.g. efflorescence, encrustation, biocolonization). Both can be caused by chemical, physical and biological weathering processes.

Of all types of weathering, black crusts are among the best known and most studied (e.g. Siegesmund *et al.*, 2007; Barca *et al.*, 2010). Black crusts are sulfate encrustations on building stones in polluted urban environments, which consist mainly of gypsum crystals but can also incorporate other salts, airborne dust, particulate matter and micro-organisms. The typical structure of such a crust contains a superficial black layer and a subsurface gypsum alteration zone. Underneath this crust, local chemical and physical alterations, e.g. cracks, may affect the original stone material. The deeper parts without alteration represent the sound stone. Black crusts develop on rain-sheltered surfaces due to the reaction of sulfur oxides in the air with calcium carbonates in the stone or mortars in the presence of water and catalyzing air pollutants. On surfaces exposed to rain, black crusts will eventually be washed off due to the moderate solubility of gypsum. Initially, although having tremendous effects on the aesthetic appearances of a building, these black crusts may indurate and thus stabilize the stone surface. However, the crusts are known to detach through time due to salt or frost action or thermal expansion, hence exposing a more vulnerable surface for further decay. Moreover, black crusts are often experienced as an undesirable expression of stone damage. Therefore, they are often removed by cleaning during restoration works, which could be an enhancement of natural weathering processes.

Restoration works which yield stone cleaning, however, should be done with care and knowledge. Therefore a specific case-study, considering the exact stone type and correct environmental conditions is appropriate, even though there is a lot of general knowledge about black crusts.

Most studies on black crusts are performed on 'pure' limestone (e.g. Török *et al.*, 2004; Fronteau *et al.*, 2010). This paper presents a structural characterization study of a gypsum crust on an arenaceous limestone, with current and advanced methods which can provide added value (Török & Přikryl, 2010). The material under investigation is the Lede stone, on which black crusts were already described (Larbi *et al.*, 2003; Quist, 2011). Traditional methods such as optical microscopy and scanning electron microscopy are combined with more innovating techniques such as X-ray fluorescence mapping and X-ray computed microtomography. The latter provides 3 dimensional insights on the stone structure in a non-destructive manner and allows for a zonation of the structural elements at the stone's surface.

2. Materials

The material under investigation is a quartz-rich limestone from the north-western part of Belgium, known as the Lede stone or Balegem stone. It originates from the sandy deposits of the Lutetian (Eocene) Lede Formation where consolidation occurred at 1 to 3 specific horizons and gave rise to discrete stone banks of several decimeter thickness. At outcrop regions, these banks occur amongst unconsolidated sediments and provided the local source of durable building material. It is used frequently in cultural heritage of northern Belgium and The Netherlands. The stone can be classified as a quartz-rich packstone to grainstone with varying amounts of micrite matrix and microsparite cement and fossil fragments. Glauconite is present in a low percentage. The Lede stone is greyish, but acquires a typical rust-colored patina in buildings.

The weathered specimens were collected at the Sint-Salvator church in Wieze (Belgium) from the well-ventilated top of the tower where they were protected against direct rain impact. In these conditions, a thin black crust developed on the stone surface.

2. Methods

2.1 Optical microscopy

2D petrographical descriptions of the samples were carried out on polished 30 µm thin sections using a Zeiss Axioscope. The samples were imbedded in a resin before analysis, to which a yellow fluorescent dye (EpoDye) was added to visualize the pore structure and could indicate the presence of microporosity.

2.2 X-ray computed microtomography

X-ray computed tomography (µCT) for 3D imaging and structural quantification was carried out at the "Centre for X-ray Tomography" at the Ghent University (UGCT) with a laboratory device (Masschaele *et al.*, 2007). The images were processed with the in-house developed software for reconstruction (Octopus) (Dierick *et al.*, 2004; Vlassenbroeck *et al.*, 2007). Afterwards, the pore structure (including cracks) were thresholded and analysed with the software program Morpho+ (Brabant *et al.*, 2011). High-energy X-ray radiographs were also collected at AB Vinçotte.

2.3 Schmidt hammer

A Schmidt hammer for concrete testing from Lasertopo BVBA was used to measure the relative rock strength along the surface of a sample.

2.4 2D X-ray Fluorescence

X-ray Fluorescence (XRF) was performed with an EDAX-EAGLE III µ-probe at the X-ray Microspectroscopy and Imaging Group from the Ghent University. The spectra were recorded in vacuum with a LN2 cooled Si(Li) energy dispersive detector. An area of 5.1 mm x 9.1 mm with both crust and stone material was mapped (40kV, 11s LT) with a resolution of approximate 100 µm.

2.5 Loss on Ignition

Three superficial crust samples were subjected to Loss on Ignition for determination of organic matter as it is often stated that black crusts incorporate organic particles. After heating the samples up to 105°C, the weight of the samples was

determined and subsequently they were heated to a temperature for 550°C for 2h to allow organic matter to combust. Subsequent weight loss was ascribed to organic matter (Heiri *et al.*, 2001).

3. Results

3.1 Petrographical analysis

Thin sections of the sample reveal the typical structure of a black crust as shown in Figure 1. A superficial black layer can be observed. It is very thin, approximately 10 µm thick, and consists of encrusted material, such as a wind-blown very fine silt fraction and particulate matter, which colors it black. Below this superficial layer, there is a zone of chemical alteration with an average thickness of 50 µm. It consists of authigenic stone material with a progressive dissolution of carbonates and precipitation of gypsum (Figure 1), which is bordered by an alteration front. In detail, it can be observed that crystallization occurs at the quartz-sparite interface. In this way, quartz grains are detached from the sound stone and incorporated in the gypsum matrix, while the carbonate cement is progressively dissolved. Porcelaneous forams form a second nucleation site for gypsum precipitation. Their microporous wall seems to be susceptible for the in situ replacement of carbonates by gypsum.

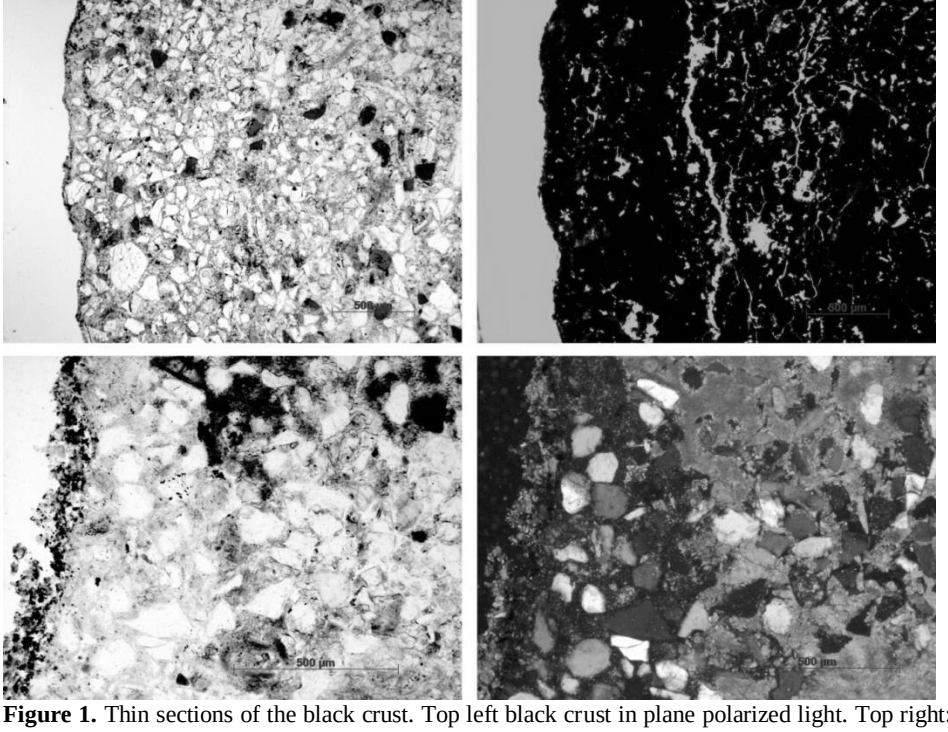

Figure 1. Thin sections of the black crust. Top left black crust in plane polarized light. Top right: same section with the bulk given in black and porosity given in grey. One large and several small cracks are visible. Bottom left: zoom on the black crust in PPL. Three zones are distinguishable: a topmost black layer with encrusted material. Secondly, just below the topmost layer, a gypsum

alteration zone, with crystalline gypsum and detached stone patches or individual quartz grains. Below this second zone, the sound stone is visible. Bottom right: same section in XPL.

Cracks can be observed in the crust and below (Figure 1, top right). Small cracks occur throughout the sample's surface. They penetrate the zone with gypsum alteration and continue into the sound stone. The cracks are sub-parallel orientated to the surface and follow grain boundaries. Infilling of these cracks by gypsum is not observed. Therefore no relation between crack formation and gypsum formation is suggested.

3.2 X-ray computed microtomography

X-ray radiographs of the stone (Figure 2) indicate the presence of a major subhorizontal crack inside the stone. This crack became visible when the stone was cut into two equal parts. A Schmidt hammer profile was taken along the cutting plane, with a 10 mm interspace (Figure 2). The rebound numbers are a measure of the rocks hardness. Normally, the higher the rebound number, the higher a rock's hardness. As these measurements are correlated within one rock, the rebound number variation can be attributed to a degree of weathering, taking into account the natural heterogeneity of the stone. Indeed, on both top and bottom side just below the weathered surface, the rebound numbers are the lowest. Especially on the top, rebound numbers increase to the inside and are doubled 30 mm below the stone surface. A decrease in rebound number is obvious around the major crack seen on the radiograph. These rebound number thus show a decrease in rock strength towards the weathered surface, but also in the center of the stone, where a major crack has developed.

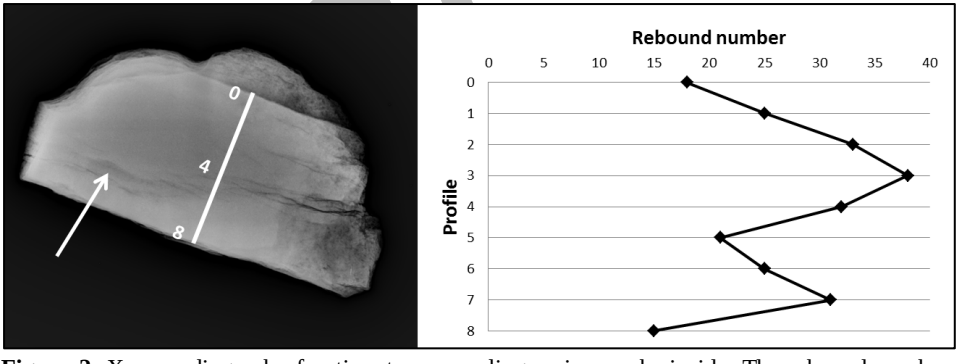

Figure 2. X-ray radiograph of entire stone revealing major cracks inside. The rebound number (Schmidt hammer) along the profile represents the relative rock's strength.

Subsamples of different sizes (Ø 10 mm, 3.4 mm & 1.8 mm) were drilled perpendicular to the weathered surface and subsequently analyzed with µCT. The structure of the upper millimeter can be seen on Figure 3, where three zones can visually be distinguished: zone 1, 2 and 3. The topmost zone 1 of the crust contains small particles and a high porosity. Zone 2 has a lower porosity than zone 1 and based on their shape, quartz grains can be recognized. The intergranular space in this zone is filled with a matrix with low grey value (Figure 3). Zone 3 consists of similar quartz grains as zone 2, but the intergranular space is filled with a matrix with a relatively higher grey value

than zone 2 and some cracks are visible. These three zones might be recognized in a partial porosity profile, with zone 1 having the highest detectable porosity, zone 2 the lowest and zone 3 a porosity which correspond most to the sound stone's porosity with local higher values due to the presence of cracks (Table 1).

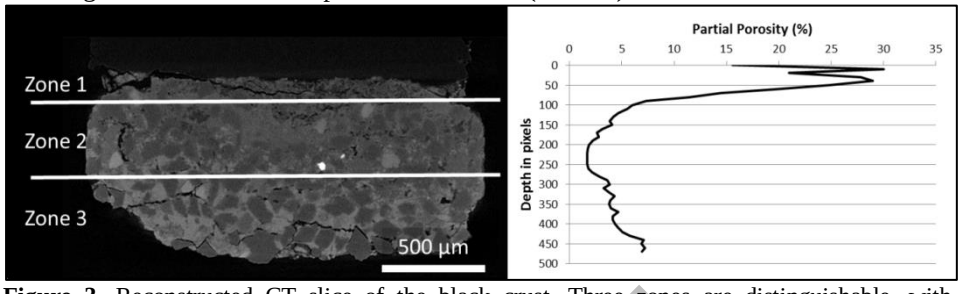

Figure 3. Reconstructed CT slice of the black crust. Three zones are distinguishable, with different porosity and grey values; the topmost layer with high porosity and very fine grained material (zone 1); a second layer with quartz grains (lowest grey value), calcite patches (high grey value) and a gypsum matrix (intermediate grey value) (zone 2) and a third layer with quartz grains and calcite cement of which the grey value is similar to the same material in zone 2 (zone 3). Cracks are clearly visible inside the stone, throughout the three zones.

Zone	Porosity
Zone 1	23,93%
Zone 2	2,72%
Zone 3	5,12%

Table 1. Average porosity of zones referred to in Figure 3.

The orientation of the main cracks was calculated and visualized in a stereographic projection by their poles to planes according to Brabant *et al.* (2011) (Figure 4). The three cracks observed in the smallest sample, being less than two millimeters below the surface, plot almost horizontal. In essence, this means parallel to the surface. The cracks occurring in the bigger sample are deeper below the surface. These show a more inclined orientation towards the surface and penetrate deeper inside the stone.

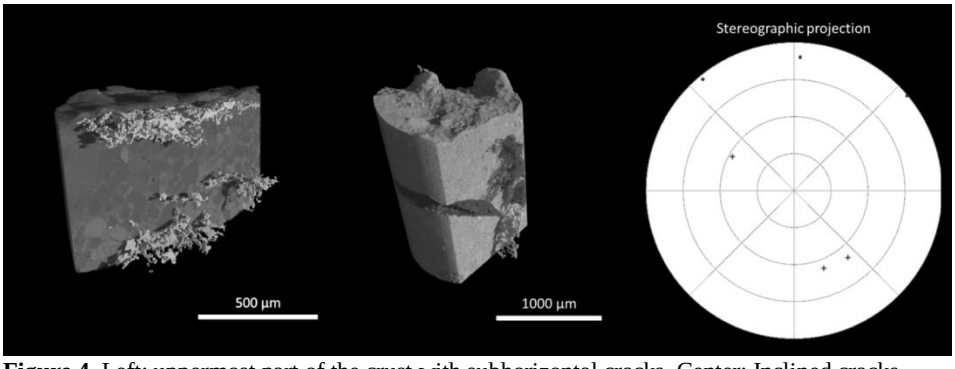

Figure 4. Left: uppermost part of the crust with subhorizontal cracks. Center: Inclined cracks deeper inside of the stone. Right: stereographic projection according to Brabant *et al*. (2011). The dots represent a horizontal orientation of the uppermost cracks, the crosses indicate a more inclined orientation for the deeper cracks.

3.3 Loss on Ignition and 2D X-ray Fluorescence

Loss on Ignition shows an average 1.0347 weight-% of organic matter present in the crust (Table 2). An elemental distribution map was obtained by µ-XRF mapping as seen in Figure 5. On these elemental distribution maps, a clear distinction between a superficial crustal layer and the more inner sound stone can be seen. The crustal layer is enriched in sulfur, phosphorus, and iron, while it is depleted in silica and calcium relative to the sound stone.

Sample	Sample Weight (g) (105°C)	Weight Loss (g) (550°C)	Weight-% OM
1	2.5122	0.2247	0.9555
2	4.031	0.2299	0.9717
3	4.8846	0.2954	1.1748
Total/Average:	11.4278	0.7500	**1.0370**

Table 2. Results obtained from Loss on Ignition.

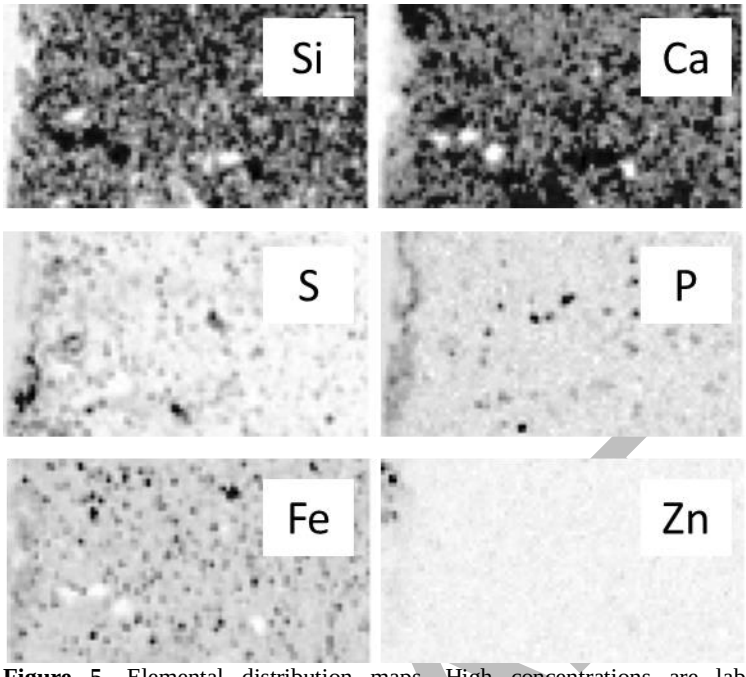

Figure 5. Elemental distribution maps. High concentrations are labeled in black, low concentrations in white. The crust is located on the left of the distribution map. The field of view is approximately 5.1 x 9.1 mm.

4. Discussion

4.1 Sound stone

The XRF data confirm the high silica (quartz grains) and calcium (fossils and cement) content of the stone. For the grain sizes exceeding the resolution (medium-fine sand fraction and fossils), high calcium correspond to low silica zones and vice versa, representing quartz grains and bioclasts. There is also a correlation in potassium, iron and silica, representing the glauconite content, although less clear due to the small grain size.

4.2 Weathering forms

The typical structure of a black crust can be observed: both thin section and µCT slices reveal a superficial encrusted black layer (zone 1), a subsurface gypsum alteration zone (zone 2) which is separated from the sound stone by the alteration front (zone 3). The average thickness of zone 1 and zone 2 together is approximately 100 microns and thickness rarely exceeds 200 microns. Cracks however, propagate throughout zone 1 and 2 into zone 3. X-ray images reveal cracks occurring in the sound stone, which have an inclined orientation towards to surface. This means they go deeper inside the stone. The cracks probably originate from physical stress induced by for example freeze-thaw cycles, as no relation between the formation of cracks and the gypsum alteration is

observed with optical microscopy and µCT. However, the alteration zone plugs the surface and therefore protects the cracks from exposure.

Since gypsum has a moderate solubility, zone 1 and 2 could lose their strength and detach when this is exposed to water impact. Furthermore, cracks in zone 1 and 2 are parallel to the surface and therefore favor the instability of these zones. When these zones would be removed, the exposed sound stone (zone 3) will probably not have the same performance as the original stone material due to the presence of cracks. These have an inclined orientation and thus expose the inner stone more to the surface, which probably results in a lower durability. Locations where cracks become exposed towards the surface will thus be zones of preferential weathering. This may explain the formation of the major crack throughout the entire inside of the stone. It is the result of progressive deeper penetration of the cracks due to contact with the surface on places where zones 1 and 2 were already detached.

µXRF data supplies additional chemical information. It reveals an enrichment in sulfur, phosphorus and iron and local zinc in the crust and a depletion of silica. The sulfur enrichment can be assigned to this gypsum. Inside the stone, there are some sulfur spots which can be attributed to secondary gypsum formation or to the mineral content. Only pyrite, observed in thin section, can cause a sulfur signal. This seems not the case however as the sulfur signal does not correlate with the iron signal and as the pyrite crystal sizes are an order of magnitude smaller than the XRF mapping resolution. Indeed, XRF measurements on the sound stone do not show these sulfur spots. So besides forming a superficial crust, gypsum also crystallized deeper inside the stone. The source of this sulfur is probably air pollution with SO_2 (Smith *et al.*, 2004). Release of sulfur by pyrite oxidation in the stone can only play a minor role as the pyrite amount is very low.

Distinct phosphorus enrichment is also seen in the crust. This was not detected with XRD, suggesting this phosphorus is not a crystalline material. The origin of this phosphorus enrichment is most probably due to biologic activity, such as algae growth or pigeon excrement. This phosphor enrichment is only superficial and seems to do no harm to the stone.

The iron enrichment in the crust is less pronounced. This probably relates to a rusty patina formation, which is usual for the Lede stone. This patina is overprinted by the black crust, but is sometimes slightly visible beneath the crust in places where the crust is damaged. The patina is formed by iron oxyhydroxides which form after oxidation and leeching of the iron inside the stone. The most probable sources are glauconite grains as these minerals weather when a stone is exposed to atmospheric conditions. This weathering is observed in thin section when glauconite grains show cracks with the formation of brownish oxyhydroxides around the surface and in the cracks of the glauconite. Minor sources might be pyrite crystals and iron content of the carbonate cement. The origin of the local zinc signal is unclear. A possible source for this zinc deposition is earlier leeching from a nearby gutter.

5. Conclusions

The weathered stone surface can be divided in three major zones which correspond to the generic black gypsum crust structure: a superficial black layer with encrusted material, a subsurface gypsum alteration zone and the sound stone. Cracks propagate throughout the different zones and are connected to the inner surface. This is clearly

visualized by µCT images. An orientation plot showed that cracks which occur close to the surface are parallel to this surface, while cracks deeper inside the stone have an inclined orientation with respect to the surface. When exposed, these cracks can act as preferential transport ways to bring the inside of the stone in contact with the environment. With the aid of fluorescent microscopy and µCT, the porosity of the different zones could be assessed and compared. The gypsum alteration zone shows the lowest porosity due to the crystallization of gypsum which plugs the pores. Therefore, it protects the inner stone from exposure along the cracks. However, on places where this plugged zone is breached by for example detachment along the superficial cracks, the cracks provide pathways for preferential infiltration. Weathering will occur more severe along these pathways. This results in the major crack which is visible throughout the center of the sample.

The superficial layers, called zone 1 and zone 2, are thin (< 200 µm), bounded by gypsum and perforated by cracks. Therefore, they can be detached by dissolving the gypsum or the creation of physical forces in the cracks by e.g. freeze-thaw action. Cleaning interventions by contractors also leads to the removal of these zones. They will enhance natural weathering process without further interaction.

Acknowledgements

Maarten Van Landeghem and Philippe Depotter from Bressers BVBA are acknowledged for the access to the renovation site at Wieze. We are grateful to dr. Geert Silversmit for the µ-XRF mapping. We thank AB Vinçotte for the use of their X-ray radiograph system.

References

Barca, D., Belfiore, C.M. et al. 2010. 'Application of laser ablation ICP-MS and traditional techniques to the study of black crusts on building stones: a new methodological approach'. *Environmental Science and Pollution Research*, **17**(8): 1433-1447.

Brabant, L., Vlassenbroeck, J., et al. 2011. 'Three-Dimensional Analysis of High-Resolution X-Ray Computed Tomography Data with Morpho+.' *Microscopy and Microanalysis*, **17**(2): 252-263.

Dierick, M., Masschaele, B. and Van Hoorebeke, L. 2004. 'Octopus, a fast user-friendly tomographic reconstruction package developed in LabView®'. *Measurement Science and Technology*, **15**(7): 1366-1370.

Fronteau, G., Thomachot-Schneider C., et al. Eds. 2010. 'Black-crust growth and interaction with underlying limestone microfacies.' *Natural Stone Resources for Historical Monuments*. London, Geological Society.

Heiri, O., Lotter, A.F., Lemcke, G. (2001). 'Loss on ignition as a method for estimating organic and carbonate content in sediments: repoducibility and comparability of results.' *Journal of Paleolimnology*, **25**: 101-110.

Kourkoulis, S. K. (ed) 2006. *Fracture and Failure of Natural Building Stones: Application in the Restoration of Ancient Monuments*. Springer, Dordrecht, The Netherlands.

Larbi, J.A., van Hees, R.P.J., Naldini, S. 2003. 'Microscopic study of weathering of white Flemish stone from the monumental Church of Our Lady in Breda, The Netherlands.' *HERON*, Special Issue. **48**(3).

Masschaele, B.C., Cnudde, V., Dierick, M., et al. 2007. 'UGCT: New X-ray Radiography and Tomography Facility'. *NIM A*, **580**(1):266-269.

Přikryl, R. and Smith, B. J. (eds) 2007. *Building Stone Decay: From Diagnosis to Conservation.* Geological Society, London, Special Publications, 271.

Siegesmund, S., Weiss, T., Vollbrecht, A. (eds) 2002. *Natural Stone, Weathering Phenomena, Conservation Strategies and Case Studies*. Geological Society, London, Special Publications, 205.

Siegesmund, S., A. Torok, et al. 2007. 'Mineralogical, geochemical and microfabric evidences of gypsum crusts: a case study from Budapest.' *Environmental Geology*, **52**(2): 369-381.

Smith, S. J., R. Andres, et al. 2004. 'Historical Sulfur Dioxide Emissions 1850-2000: Methods and Results.' *PNNL, JGCRI Research Report, PNNL-14537.*

Török, Á. and Rozgonyi, N. 2004. 'Morphology and mineralogy of weathering crusts on highly porous oolitic limestones, a case study from Budapest'. *Environmental Geology*, **46**(3): 333-349.

Török, A. and Prikryl, R. 2010. 'Current methods and future trends in testing, durability analyses and provenance studies of natural stones used in historical monuments'. *Engineering Geology*, **115**(3-4): 139-142.

Vlassenbroeck, J., Dierick, M., Masschaele, B., et al. 2007. Software tools for quantification of X-ray microtomography at the UGCT, Nuclear Instruments and Methods. In: Physics Research Section A: Accelerators, Spectrometers, Detectors and Associated Equipment, Volume **580**, pp. 442–445.

Winkler, E.M., 1994. *Stone in Architecture: Properties, Durability*, 3rd edn. Springer-Verlag, Berlin Heidelberg, Germany.